Collective optical effect in complement left-handed material

S.-C. Wu, C.-F. Chen, W. C. Chao, W.-J. Huang and H. L. Chen,
National Nano Device Laboratories,
1001-1 Ta-Hsueh Road, Hsinchu,
Taiwan R.O.C

A.-C. Hsu and J.-L. Chern
Institute of Electro-Optical Engineering,
National Chiao Tung University,
1001, Ta-Hsueh Road, Hsinchu, Taiwan

Abstract: The Babinet's effect occurs at a long wavelength span of incident light during FTIR (Fourier Transform Infrared) spectroscopy scanning in complementary LHM (Left-Handed Material) samples. The occurring wavelength ranges from 4 to 20 μ m under a scanned light source in 2.5~25 μ m regime. The LHM sample consists of an SRR (Split Ring Resonator) adjacent to wire array in periodic order. Complement samples were prepared using standard integrated-circuit processes on a Si wafer. Gold nano particles were deposited on the conducting parts of patterns. The positive pattern is a sample that patched with periodic Au wire on the Si wafer. And the negative one is adopted with a reverse way, the wire part is empty of Au and the surrounding space is filled with Au particles.
Transmittance-enhanced behavior was identified from those consequent data. The surface plasmon resonated effect on Au nano particle on top of surface seems to contribute the enhancement.

Key-words: Babinet's effect, Left-Handed Material, Gold nano particle.

1. Introduction

In the advent of nano era, all technologies step into mini-size world to get the biggest benefits by scale reduction. Especially, in IC industry, the bigger wafer and the smaller size are adopted, the larger competing and income can be made. Meanwhile, there are some of distinct effects will emerge simultaneously under dimension of device through a big step shrunk. In IC devices, they exist the parasitic effects and even quantum phenomena, which more or less influence on the devices performance. Therefore it is urgent needed to evaluate the circuit behaviors using simulation methods during design processes. On the other hand, in the field of optics, the device density is also increasing with the rate of communication. Thus the multifunction of optical device attracts the interest of wireless designers'. Designers hope to include laser, grating, wave-guide, coupler, sensor and other functions into a monolith and demonstrate a complete performance. The probable effects of scaling down on optics of a device are

worthy of studying. For instance, the specula phenomena involve sub-wavelength transmitting behavior [1, 2], doubly negative permeability and permittivity effects [3-5] Wood's anomaly [6], and even the Babinet's effect [7]. Babinet's effect is that the diffraction pattern on an aperture is the same as the pattern for opaque object of the same shape illuminated in the same manner. In addition, the two spectra of complementary pattern must be out of phase and have the same amplitude at each point on a detector. The transmittance enhanced is due to resonance of the surface plasmon in the metal film on top of sub-wavelength grating [8, 9]. The degree of enhancement is depending on incident wavelength [10]. Additionally, the relation between the wave vector of illuminating light and the reciprocal lattice of grating array needs to obey the momentum conservation [11]. Accordingly, the scale of wire grating is very important when the wavelength of light is reduced to IR regime, or even into visible range. It acts as an optical filter but intensity of passing light is enhanced [12]. Therefore the authors anticipate that IC technology will be further scaled down until a nano device can have a completely optical application. The LHM is a specific pattern, which indicates the unique characteristics of a negative refraction index [13]. The pattern is a combining of the SRR pattern at $\mu < 0$ and the wire grating with $\varepsilon < 0$ [14]. Therefore, FTIR is used herein to evaluate the effect of a negative index at the designed frequency. Interestingly, a comparison of FTIR spectra demonstrates the Babinet's behavior between the complementary patterns. Meanwhile, a large range of Babinet's behavior effects are observed among a long regime of incident wavelengths. This phenomenon motivates this work. The canceling behaviors of opposite responses in spectra will be investigated by overlapping the both complement patterns together. Thus, the distribution of electromagnetic field can be observed using near field probing method at polarized light. In addition, the Wood's anomaly and the transmittance enhancement due to surface plasmon resonance are also observed.

This study also involves Au nano particle with specific behaviors and unique properties [15], which are very useful in bios, optics and nano-electronics, for instance. These particles were incorporated to a fabricated LHM to elucidate new effects. Therefore this work included this technique into this LHM array fabrication and expects to find something new at this combination. A series of meta-material samples were fabricated using the mature IC technology and Au nano particle treatment. One set of results investigated by CO_2 laser has been accepted at OSA Optical Annual Meeting in 2003 [16]. The SRR patterns measured using FTIR were also presented at Aphys 2003 Conference [17]. This work addressed only the optical properties on LHM array obtained using FTIR. The description in this phenomenon will be presented following up the experiment Section 2 states the experiment and characterization details. In Section 3, we report the main results and discuss the experimental data. Section 4 draws the conclusions.

2. Experiment

The patterned samples were fabricated using standard IC (integrated-circuit) processes. The substrate was a 6" double polished n-type silicon wafer. The wafer was cleaned by RCA cleaning. Reference [17] describes negative and positive patterning of samples [16]. For positive one, the

conducting parts in the pattern are filled with Au metal. Therefore, in the negative samples, the space along the conducting parts is filled with the gold particles. The conducting parts are thus empty and not covered by Au film; only SiO_2 remains on the Si substrate. Photographs were taken using SEM (Scanning Electronic Microscopy) instruments individually. The optical microscopy tool is very hard to view the negative patterns owing to scattering effect from the gold particles.

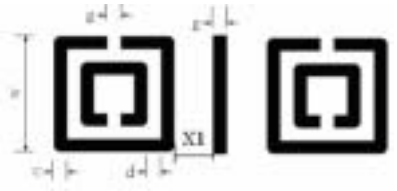

c	1
d	1.2
g	1.84
w	10.48
Y	6.8
X1	3.2

Fig.1 LHM pattern and Dimensions. (unit=μm)

Figure 1shows the size LHM array herein. The thickness of Au was ~ 20nm while the thickness of the Si substrate was ~0.7mm. The horizontal distance between the two LHM units was 3.2 μm and the vertical distance was 6.8 μm. Typically, the area of an entire LHM array sample is about 4 mm X 4 mm. An entire sample has *150*×*200*= 30,000 LHM units. The FTIR equipment used herein was QS 300 produced by Bio-Rad Laboratories, Inc. The range of wavenumbers of the light source was 4000~400 cm^{-1} (The wavelengths ranged from 2.5 to 25 μm). Each sample was obtained by carefully cutting with diamond pen. In this experiment the incident light was perpendicular to the pattern surface. Each of spectra was obtained using 16scans.The time resolution was 2 sec and the scanning length was 30 sec. The purpose of FTIR is to find out the existing components or constituents of the film deposited on Si wafer. Therefore the response of signal under such as measuring is usually adopted by intensity ratio, which is divided the response intensity of testing sample with that of pure Si wafer. It is so-called as absorption ratio during the testing sample inserted. On the other hand, it is just the absorption signal resulted from the film component top of Si wafer. But in this study, for clearly understanding, we adopted the transmittance instead of absorption to evaluate the SRR behavior.

This paper considers only the results that correspond to LHM pattern of the minimum size.

3. Results and Discussion

Figure 2 shows the SEM photographs of positive LHM array and negative one respectively. The magnifications are 1000x and 3500x in positive and negative array, respectively.

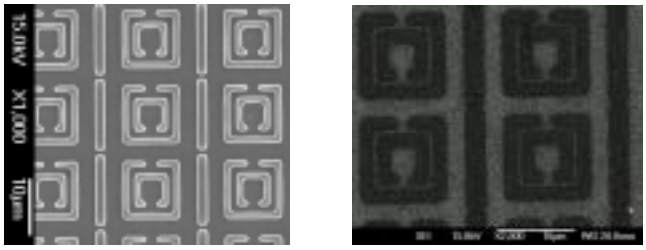

(a) (b)

Fig. 2. SEM photographs of LHM array pattern 1000x in positive pattern (a), 3500x in negative pattern (b).

Figure 3 displays the FTIR transmittance spectra of both LHM patterns. Babinet's behaviors are obvious in many regions. The range of wave numbers is from 696~710 cm^{-1} (14.1~14.4 μm), to 2926 cm^{-1} (3.4 μm). Babinet's behavior is clearly exhibited in over 25 positions. In order to further showing the relationship of the complementary behavior, the FTIR spectra were zoomed in at two regions. One region is at 600~3000 cm^{-1} shown as Fig. 4, and another at 1200~2800 cm^{-1}.exhibited as Fig. 5, respectively. At those regions, the transmittance (T) values are taken to be $T_p(\lambda) = T_0(\ ) \pm \Delta T(\lambda)$ and $T_n(\lambda) = T_0(\lambda) \pm \Delta T(\lambda)$ for that of

positive and negative LHM patterns, respectively. T_p (λ), and T_n (λ) are the peak or valley transmittance values of the positive and negative patterns in the regions of Babinet's effects, and T_0 is the approximate transmission of the undiffracted light, which is considered to be the average value of T_p (λ)+ T_n (λ). Some T_0 values exceed 100%, probably because of the effect of transmission enhanced on both types of patterns. Where ΔT (λ), i.e., the difference between T_n and T_0, or T_p and T_0, is derived from the difference in diffraction from opaque obstacles in both SRR patterns.

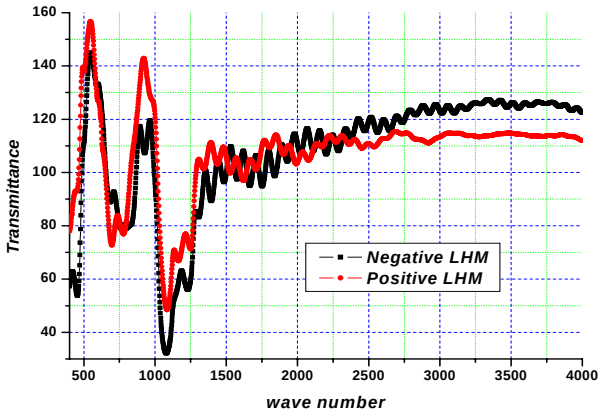

Fig. 3. (Color) FTIR transmittance spectra of both types of LHM patterns. Wavelength span at incident light source is 400~4000 cm^{-1}.

Notably, the complementary behaviors of the spectra are very clear at some wavelengths. For instance, at around 700, 1220, 1393, 1444, 1530, and 1800 cm^{-1}, the phase differences between waveforms are almost equal to π. On the other hand, it is seldom found that Babinet's behavior is still exhibited under a sophisticated and periodic patterned array. Especially the incident wavelength is also compatible with the size of array. The annihilation effect of precise overlapping of two reciprocal patterns is thus observed. This finding is being investigated and will be discussed in a later study.

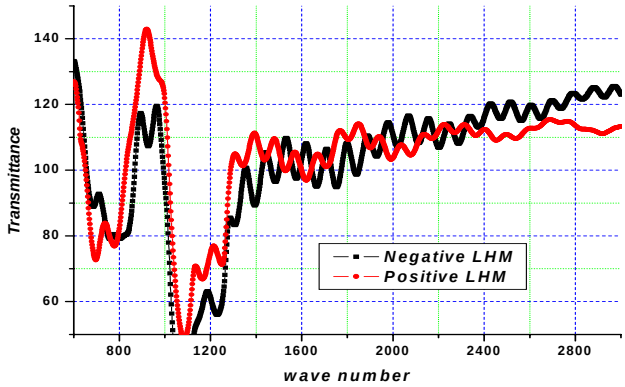

Fig. 4. (Color) Magnified spectrum of FTIR data that clearly shows the Basinet's effect in the 600~3000 cm^{-1} regime.

Wood [18] and Fano [19] described maximum and minimum of the diffracted light at metal grating experiments. Therefore the x and y dimension of the LHM array are examined to elucidate the relationship of anomaly with the array dimension. The contribution of the surface plasmon (SP) to the enhancement of transmittance at this peculiar wavelength due to resonance with the incident light is also considered.

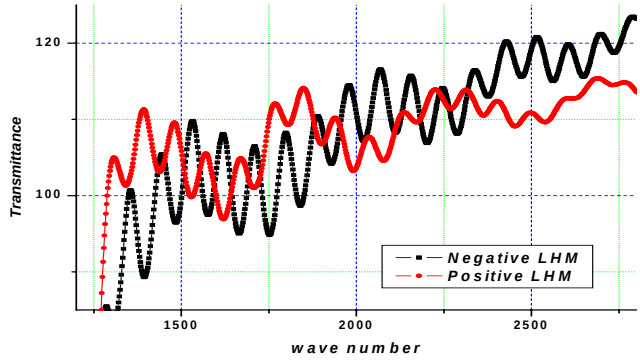

Fig. 5. (Color) Magnified spectrum of FTIR data that clearly shows the Basinet's effect in the 1200~2800 cm^{-1} regime.

In the mid-IR region, the dielectric parts can be recognized as holes, as in other work [20] in the visible regime. Therefore, the model of the coupling of light with an SP on a periodically

corrugated metal surface is consistent with the conservation of momentum, as described in [21]. That is, $K_{sp} = K_x + iG_x + jG_y$, where the K_{sp} is the SP wave vector, $K_x = \hat{x}(2\pi/\lambda)\sin\theta$ is the $\hat{x}$ component of the incident light's wave vector, and G_x, G_y are the reciprocal lattices for a rectangular-lattice vectors with $G_x = 2\pi/a_x$, $G_y = 2\pi/a_y$; i, j are integers. Where a_x and a_y are the lattice constants of the unit cell of array in x-axis and y-axis, respectively. The θ value is 0 under normal incident. The SP dispersion [9] is given by

$$\left|K_{SP}\right| = \frac{\omega}{c}\left\{\left[\varepsilon_m \varepsilon_d /(\varepsilon_m + \varepsilon_d)\right]^{\frac{1}{2}}\right\},$$

where ω is the angular frequency of the incident light, ε_m is the real part of the dielectric constant of the metal, and ε_d is that of dielectric material. In our case, the incident light is in mid-inferred regime, whereas the value of ε_m in Au metal [22] is negative and very larger than ε_d . That is, the value of K_{SP} can be simplified to a formula of ε_d and the reciprocal vectors. The refraction index n is not a fixed value under the range of mid-IR [23]. Especially at the region of 6~10μm, the refraction index n is decreasing with wavelength increasing, herein the n value can down to 0.11. Therefore, in this work, we used the value 1.9 as refraction index value of SiO_2 to predict the SP resonate wavelength. And the values of a_x and a_y are 19.76 μm and 17.28 μm, respectively, in the sample. Accordingly, there can exhibit many of the resonated behaviors of SP under wavelength of 25μm. Under the condition $|i| + |j| = 1$, the resonance at the Au/SiO_2 interface is at a wavelength greater than 25 μm and is therefore invisible. Where i and j are the Miller indices associated with the x and y-axes, respectively. The most distinct peak at 18.28 μm in the positive and negative patterns corresponds to the resonance of the surface plasmon in the interface of the air and the Au. The value of this peak is consistent with the calculation made using the SP formula. The other peaks at 10.9 μm in the positive pattern and 10.4 and, 11.2 μm in the negative pattern follow from the $|i| + |j| = 2$ condition at the Au/SiO_2 interface. When the sum $|i| + |j|$ exceeds 3, the corresponding wavelength will be smaller than the lattice dimensions of the wire array. Thus the diffraction behavior is likely to be exhibited in this region. The resonance is also too weak to be manifest under this higher order condition.

The dispersion of Au nano particles on the conducting surface in array pattern was observed using SEM. The distribution of Au particles is like that of cluster in a semicontinuous metal shown as Fig. 6. Accordingly, the Au nano particles contribute to the enhancement of transmittance due to percolation-enhanced nonlinear scattering (PENS) effect [24]. Because the metal line in positive LHM array or surrounding parts in negative one are of same effect as semicontinuous metal film. Thus the local field E could be enhanced with the collective plasmon resonance under ensembles of metal particles [25].

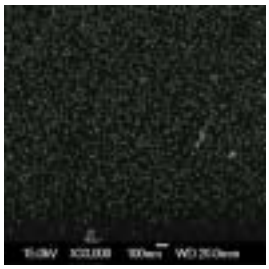

Fig. 6 SEM photograph of dispersion of Au nano particle on conducting surface in LHM pattern.

Hereon, we can also find out the phenomena of maxima and minima in spectrum that called as Wood's anomaly [18] as Fig.3. These anomalies now are well known since the work of Fano [19], that are due to the excitation of surface plasmon propagating along the metallic-dielectric interface. In fact the conditions for the occurring of Wood's

anomaly are similar with SP resonance, except that the wave vector of the grazing light replaces Ksp. The magnitude of this wave vector is $k_{diff} = 2\pi n_d/\lambda$, where $n_d = \varepsilon_d^{1/2}$. In normal incident these wavelength are given by

$$\lambda_{max}(i, j) = \frac{a_0}{\sqrt{i^2 + j^2}} \left(\frac{\varepsilon_m \varepsilon_d}{\varepsilon_m + \varepsilon_d}\right)^{1/2}$$

$$\lambda_{min}(i, j) = \frac{a_0}{\sqrt{i^2 + j^2}} \sqrt{\varepsilon_d}$$

The loci of Wood's anomaly is almost following with the SP dispersion branches in the (E, k_x) diagram, and the minima occurring at slightly shorter wavelength than the maxima. Two dip valley positions around 21.8 μm in spectra of positive and negative patterns are due to the Si-O-Si bond bending motion and can find from the FTIR data sheet.

Transmittance enhanced factor can be evaluated based on the true area ratio of conducting part in LHM to the complete area in our sample. The area ratio of the positive pattern is 0.22, explaining what the enhancement factor for the highest peak is about 2. However, it is around 6.6 for the negative pattern. The non-coherent irradiating light thus has a marked effect, which may be more obvious when polarized coherent light source is used. This claim is being investigated further.

4. Conclusion

Complimentary LHM patterns were fabricated to include Au nano particles by standard IC processes. More than 25 Basinet's effects were observed over a wide range of wavelengths. Interestingly, some complementary waveforms arise in the same positions. This result has seldom been reported and should be studied further. Whether the complementary spectra could be added together to yield a flat response was also investigated. Other novel properties such as enhanced transmittance behavior, and Wood's anomaly associated with SP resonance were observed. The SP resonated positions for both types of pattern were also found out from the FTIR scanning and able to check with referring formula. In there, some deviations exist due to variation of dielectric constant. The enhanced factor of the negative array exceeds that of the positive one, although the surface of the former is covered with more gold particles. Therefore the collective localized electric field, enhanced by Au nano particles, can combine with the surface plasmon to increase transmittance. Therefore further investigation is needed, particularly in the field distributed over the conductor in both types of LHM array.

By the way, the FTIR measurement can fast evaluate the optical properties of the pattern itself. The substrate effect will fully eliminate while the substrate was adopted for background.

Acknowledgement: The authors would like to thank the National Science Council of the Republic of China, Taiwan for financially supporting this research under Contract No. NSC92-2215-E-492-009.

References:

[1] A. K. Sarychev, et.al., Resonance transmittance through a metal film with subwavelength holes, IEEE J. Quantum Electronics, 38, 7, 2002, pp 956-963.

[2] T. W. Ebbesen, et.al., "Extraordinary optical

transmission through sub-wavelength hole array", *Nature*, 391, 1998, pp.667-669.

[3] R. A. Shelby, et.al, Experimental verification of a negative index of refraction, Science, 292, 2001, pp77-79.

[4] P. Gay-Balmaz, et.al, Electromagnetic resonances in individual and coupled split-ring resonator, J. Appl. Phys. 92 ,5, 2002, pp2929-2936.

[5] C. Caloz, et.al, Full-wave verification of the fundamental properties of left-handed materials in waveguide configurations, J. Appl. Phys. 90, 11, 2001, pp5483-5486.

[6] R. W. Woods, Anomalous Diffraction Gratings, Phys, Rev. 48, 1935, pp928-936.

[7] M. Babinet, Memories d'optique meteorologique, C. R. Acad. Sci. 4, 1837, pp638-648.

[8] U. Schroter and D. Heitmann, Surface-Plasmon-enhanced transmission through metallic grating, Phys, Rev. B, 58, 23, 1998, pp15419-15421.

[9] M. B. Sobnack, et.al., Stationary surface plasmons on a zero-order metal grating, Phys. Rev. Lett. 80, 25, 1998, pp5667-5670.

[10] T. Lopez-Rios, et.al, Surface Shape resonances in lamellar metallic gratings, Phys. Rev. Lett. 81, 3, 1998, pp665-668.

[11] W. L. Barnes, et.al., Physical origin of photonic energy gaps in the propagation of surface plasmons on gratings, Phys. Rev. B, 54, 9, 1996, pp6227-6244.

[12] J. A. Porto, et.al, Transmission resonance on metallic gratings with very narrow slits, Phys. Rev. Lett. 83, 14, 1999, pp2845-2848.

[13] R. A. Shelby, et.al., Experimental verification of a negative index of refraction, Science, 292, 2001, pp77-79.

[14] J. B. Pendry, et.al, Extremely low frequency plasmons in metallic mesostructures, Phys. Rev. Lett. 76, 25, 1996, pp4773-4776.

[15] X. M. Lin, et.al, Direct patterning of self-assembled nanocrystal monolayers by electron beams, Appl. Phys. Lett. 78, 13, 2001, pp1915-1917.

[16] A-Chuan Hsu, et.al.," Far-infrared absorption of split ring resonators:" OSA Optical annual meeting accepted (2003)

[17] S.-C. Wu, et.al., Fast evaluating the novel optical properties of Split Ring Resonator by FTIR, accepted by First international Meeting on Applied Physics 2003.

[18] R. W. Wood, Phys. Rev. 45, 1935, pp928-938.

[19] U. Fano The theory of anomalous diffraction gratings and of quasi-stationary waves on metallic surfaces (Sommerfeld's waves) J. Opt. Soc. Am. 31, 1941, pp213-222.

[20] L. Martin-Morenno, et.al, Theory of extraordinary optical transmission through subwavelength hole array, Phys. Rev. Letts. 86, 6, 2001, pp1114-1117.

[21] T. J. Kim, et.al, Control of optical transmission through metals perforated with subwavelength hole array, Opt. Lett. 24, 4, 1999, pp256-258

[22] H. Raether, Surface Plasmons on Smooth and Rough Surfaces and on Gratings, Springer-Verlag, Berlin, 1988.

[23] E. D. Palik, Handbook of Optical Constant of Solids, Academic, Orlando, 1985.

[24] V. M. Shalaev and A.K. Sarychev, Nonlinear optics of random metal-dielectric films, Phys. Rev. B, 57, 20, 1998, pp13265-13288.

[25] A.K. Sarychev, V. A. Shubin, and V. M. Shalaev, percolation-enhanced nonlinear scattering from metal-dielectric composites, Phys. Rev. E, 59, 6, 1999, pp7239-7242.